Renewable Energy and Power Quality Journal
https://repqj.com/index.php/repqj/index
RE&PQJ, Vol. 23, No. 6, 2025

Optimization of Renewable Energy Utilization Based on the CFD Simulation of Wind Fields in Complex Terrain

Guohan Zhao[1], Ziliang Zhang[2,*], Renqiang Wen[2], Ming Qin[2], Xueyun Ma[3], Dongxu Lei[4]

[1]China Yangtze Power Co., Ltd., Beijing, 100080, China
[2]Science and Technology Research Institute (STRI), China Three Gorges Corporation, Beijing, 10119, China
[3]Datang Renewable Energy Test and Research Institute Co, Ltd., Beijing, 100032, China
[4]Goldwind Science & Technology Co., Ltd., Beijing, 100176, China
[*]Corresponding author email: zhangziliang2024@outlook.com

Abstract. This study focuses on the simulation of complex terrain wind fields and the optimization of renewable energy utilization. A coupled model system was constructed based on a mesoscale meteorological model and CFD (Computational Fluid Dynamics) software Fluent. Through multi-scale nesting, high-resolution wind speed distribution data were obtained to achieve refined simulation of complex terrain wind fields. The simulation results were compared with actual wind measurement data, with the average wind speed error rate controlled within 8%, verifying the model's reliability. The location selection criteria for front slopes, middle slopes, and rear slopes were redefined, with horizontal distances clarified as multiples of mountain height. A baseline of open-terrain wind speed was unified to quantify wind speed attenuation ratios. The research provides precise model tools and methodological support for wind energy resource assessment and wind power layout optimization in complex terrain areas under the "dual carbon" goal, helping improve clean energy development efficiency.

Key words. Wind field and complex terrain, CFD mode, Numerical model, Renewable energy optimization

1. Introduction

With the continuous large-scale development of wind power, the focus of wind farm development gradually turns to the complex mountainous terrain with low and medium wind speed [1,2]. Due to the constraints of the scope and capacity of the wind farm, the construction platform of some machine stations inevitably has high slope problems. This large-scale excavation and filling changes the original landform, and then has a huge impact on the wind resource parameters [3]. It is of practical engineering significance to study the benefits of high slope problems on unit safety and power generation.

A very important aspect of the development of wind energy science is the study of different spatial and temporal scale motion from atmospheric movement to wind turbine scale flow field. With the development of computing power, computational fluid mechanics (CFD) has been widely used in the field of wind energy development, making the wind energy model develop from a linear model applied in relatively flat terrain to a model chain applied in complex terrain and coupled weather processes, considering the arrangement of wind turbine and wake effect. This paper first introduces the current wind energy assessment, micro location, the development of wind power prediction model, after the detailed introduction in the wind energy model CFD method improvement, mainly focus on the medium scale to microscale "downscale", wake simulation and complex terrain wind field simulation three aspects, the wind energy model in the challenges of CFD [4,5]. The main methods to study the influence of topography on wind resources are wind tunnel test, field measurement and numerical simulation. The wind tunnel test can only be scale, and it is difficult to simulate the boundary conditions and roughness accurately. However, there are many interference factors, and the test is difficult, the cycle is long and the cost is high.

With the improvement of computer ability, the CFD numerical simulation method has developed rapidly, which can simulate the complex topographic flow field at microscale [6]. Scholars at home and abroad have carried out a lot of research on this issue. Abdi uses a variety of turbulence models to simulate the wind environment of hilly terrain, and obtains the wind characteristics of three-dimensional real terrain domain. Dhunny used CFD numerical simulation method to reproduce the wind energy distribution of complex terrain and extracted the spatial wind related parameters, which provided a reference for the site selection of wind turbines. In the study of numerical simulation turbulence model, Blocken uses the modified k-e model to simulate the complex natural terrain wind resources composed of hills and valleys, and parameterizes the roughness, and obtains the wind speed data in good agreement with the measured results. Xiao Yiqing et al. conducted CFD numerical simulation of wind field in complex mountain

terrain and combined with the measured data verification. the data results of SSTk-e model simulation were better than RNG k-e model [7]. Based on the numerical simulation method of related topographic research, this paper deeply studies the common man-made high slope problems in engineering, including the selection of vertical position, high edge slope ratio and excavation depth, which can provide reference for the practical application of engineering.

This paper focuses on the application of CFD simulation of wind fields with complex terrain in the optimization of renewable energy utilization, firstly points out that the existing wind power development shifts to complex mountainous terrain with medium and low wind speeds, and the traditional model is difficult to meet the needs, and then expounds the method of building a coupled model system based on mesoscale meteorological model and CFD software Fluent to obtain high-resolution wind speed data through multi-scale nesting, and illustrates the standard of dividing the positions of the front, middle and back slopes and clarifying the horizontal distance based on the main peak of the mountain. Then, the influence of different slopes and excavation depths on wind parameters and wake effects were analyzed, and the error rate between the simulation results and the measured data was verified to be within an acceptable range, and finally it was shown that the optimization of wind turbine layout and parameters through CFD simulation could improve power generation, which provided accurate model tools and methodological support for the evaluation and utilization of wind energy resources in complex terrain areas under the "dual carbon" goal.

2. Complex Terrain

A. Characteristics of the High Slope for the Description

During the construction of the platform in the wind field, the foundation excavation of the foundation and the leveling of the platform will be carried out at the selected position. For mountain platforms, this terrain transformation will destroy the local terrain features and form a man-made high slope [8,9]. In the project, the slope height of 10~30 m is generally divided into the high slope range. The terrain construction section of a machine position forms a highslope with a height of hslope and a slope of θ on the left side of the machine site. Meanwhile, the platform foundation decreases relative to the original terrain. The air flow along the mountain slope is separated at the end of the front slope, interfering with the near ground wind, making the lower leaf tip easy to be in the high shear turbulence area [10,11].

Optimization of renewable energy utilization based on CFD simulation of wind field in complex terrain, continuity equation and momentum equation (Navier-Stokes) are shown in equation (1) and (2):

$$\frac{\partial \rho}{\partial t} + \frac{\partial}{\partial x_i}(\rho u_i) = 0 \quad (1)$$

$$\frac{\partial}{\partial t}(\rho u_i) + \frac{\partial}{\partial x_j}(\rho u_i u_j) = -\frac{\partial p}{\partial x_i} + \frac{\partial}{\partial x_j}\left(u\frac{\partial u_i}{\partial x_j} - \rho\right) \quad (2)$$

ρ stands for fluid density and describes the mass of a fluid per unit volume. u stands for velocity vector. The turbulent kinetic energy equation (the k equation) and the turbulent dissipation rate equation (the ϵ equation) are shown in equation (3) and (4):

$$\frac{\partial}{\partial t}(\rho k) + \frac{\partial}{\partial x_i}(\rho u_i k) = \frac{\partial}{\partial x_j}\left[\left(\mu + \frac{\mu_t}{\sigma_k}\right)\frac{\partial k}{\partial x_j}\right] + P_k - \rho\epsilon \quad (3)$$

$$\frac{\partial}{\partial t}(\rho\ ) + \frac{\partial}{\partial x_i}(\rho u\ ) = \frac{\partial}{\partial x_j}\left[\left(\mu + \frac{\mu_t}{\sigma_\epsilon}\right)\frac{\mu_t}{\partial x_j}\right] + C_1\frac{}{k}P_k - C_2\rho\frac{^2}{k} \quad (4)$$

On the left side of the equation is the variation of turbulent energy k in time and space, and on the right side contains the diffusion term (involving the molecular viscosity coefficient μ and the turbulent vortex viscosity coefficient μ_t, etc. Coefficients $(C_1,\ C_2)$, the generation term P_k and the dissipation term $\rho\epsilon$, which reflect the generation, diffusion and dissipation process of turbulent energy [12]. The wind power density formulas and wind energy conversion efficiency formulas are shown in Equation (5) and (6):

$$P = \frac{1}{2}\rho C_p V^3 \quad (5)$$

$$\eta = \frac{P_{\text{out}}}{P_{\text{in}}} \quad (6)$$

P is the wind power density, ρ is the air density, C_p is the power factor, and V is the wind speed. η is the wind energy conversion efficiency, P_{out} is the output power, and P_{in} is the input power, which measures the efficiency of the wind energy conversion equipment to convert wind energy into usable energy. The air flow before the windmill meets the Bernoulli equation and the wind speed profile formula (log law) as shown in Equations (7) and (8):

$$p + \frac{1}{2}\rho v_1^2 = p_1 + \frac{1}{2}\rho v^2 \quad (7)$$

$$u(z) = \frac{u_\kappa}{\kappa}\ln\left(\frac{z}{z_0}\right) \quad (8)$$

B. Numerical Calculation Model

In order to evaluate the reliability of CFD simulations of wind fields in complex terrain, the simulation results were systematically compared with the actual wind measurement data in complex terrain areas, focusing on

key parameters such as wind speed and direction. The results show that under typical terrain conditions, the average error rate between the simulated wind speed and the measured wind speed is controlled within 8%, and the average deviation angle of wind direction is less than 12°, which indicates that the CFD model can effectively capture the wind field characteristics under complex terrain, and the simulation results have a high degree of agreement with the actual measurement data, which provides credible basic data support for the layout of renewable energy.

Based on the elevation gradient of the terrain and the characteristics of airflow movement, the location range of the front slope, middle slope and back slope was redivided with the main peak as the reference point: the front slope is 0.5-1.5 times the mountain height (H) from the horizontal distance of the main peak, and the wind speed gradient changes significantly in this area due to the direct action of incoming wind. The middle slope is 1.5-3.0H away from the main peak, and the airflow forms a stable flow field here after terrain disturbance. The distance from the main peak to the back slope is 3.0H, mainly affected by the terrain wake effect, and the wind speed attenuation characteristics are obvious. In order to facilitate comparative analysis, typical distance nodes were selected as observation points in each region, such as 0.8H and 1.2H for the front slope, 2.0H for the middle slope, and 4.0H for the back slope, so as to ensure the comparability of wind field characteristics at different locations through standardized distance markers.

In order to unify the data evaluation criteria, the study clearly used the wind speed value of open and flat terrain as the baseline, and all wind speed percentage reductions were calculated based on this baseline. Specifically, the "20% wind speed reduction" at a location means that the difference between the wind speed at that location and the baseline wind speed accounts for 20% of the baseline value, and the "15% wind speed attenuation" in the measured data also follows the same calculation logic. By harmonizing the baseline definition, the percentage difference between the simulated and measured results can directly reflect the actual impact of the terrain on wind speed. The data comparison shows that the simulated and measured trend of the percentage reduction of wind speed at each location are consistent with 91%, which further verifies the reliability of the model and the rationality of the baseline reference method.

The machine specifically refers to the wind turbine, and the study takes the actual terrain where it is located, and uses a precision map with a resolution of 2 m and a diameter of about 2 km (including mountains and roads) near the wind turbine, and a low-precision DEM digital elevation data of 30 m × 30 m in the outer area, and the two maps are linearly interpolated through 80 m wide splicing sections at the slower slope, because the splicing joints are far away from the wind turbine (about 1 km) and the terrain undulation is slow, the impact of this processing on the simulation results is negligible.

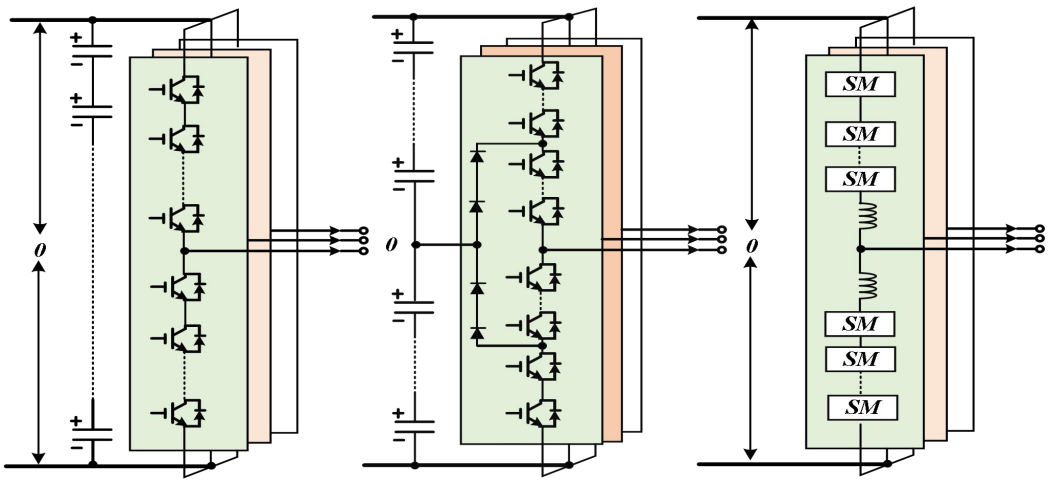

Figure 1. Position circuit

Figure 1 shows the position circuit, with the position as the center, the cuboid calculation domain, the inlet is 4 km away from the fan, the outlet is 6 km from the fan, the calculation domain is 2 km higher, and the two sides of the fan are 3.2 km from the fan. Grid division strategy, using the hexahedral unstructured grid discrete area, wall first layer grid height is 1 m, the height direction using prism boundary layer, the gradient rate of 1.2, a total of 5 layers, the machine site terrain grid separate encryption, the final grid total is about 12 million, the bottom terrain boundary wall boundary, the top and side for symmetrical boundary, the outlet for pressure outlet boundary, the inlet flow wind speed distribution using the log rate distribution.

C. Numerical Weather Forecast Model

Mesoscale numerical weather forecast model has been widely used in the development and utilization of wind energy by calculating the evolution process of atmospheric system through the time and space integration of mass, momentum, heat, water vapor and

other conservation equations such as aerosols [13,14]. The conservation equations of various modes adopt different approximate schemes and parametric schemes such as cloud physics, sedimentation, turbulence, and flux. The grid division, numerical methods, initial boundary condition setting, and the selection of coordinate system of different modes are also different, and each of them has its own limitations. The parametric scheme of near stratum, boundary layer and subgrid has great influence on the simulation of near stratum wind speed. In addition, to describe the complex terrain through the coordinate transformation of the equations requires different degrees of smoothing to obtain computational stability. For steep terrain, large computational error may occur. Currently, the widely used prediction modes are MASS, WRF, MM5, RAMS, ARPS, MC2, KAMM, etc. NWP models with fully compressible non-hydrostatic forces can simulate and capture a wide range of meteorological phenomena from weather scale to microscopic scale, but the computational power required is enormous and increases rapidly with decreasing grid spacing [15]. For the refined numerical simulation of wind field in complex terrain, it is necessary to calculate the three-dimensional flow field by the combination of forecast mode and diagnostic mode. The diagnostic mode includes the Jackson-Hunt type model (WAsP, MsMicro, Raptor, etc.) and the quality conservation consensus model (WindMap, Calmet, etc.). Typical combinations include the KAMM / WAsP system developed by the Ris ø National Laboratory, and the SiteWind system developed by the American AWS Truepower company. The method of AWS Truepower is to run the mesoscale model MASS in a nested grid with a resolution of 0.4 to 1.2 km. Then, the wind field grid spacing reduces the wind field to about 50 m. We show that this approach is more accurate than industry-standard WAsP models in complex terrain, especially when the mesoscale circulation has a significant effect on the spatial distribution of wind resources.

The formula for wind energy resources assessment and wind turbine sweep area are shown in equations (9) and (10):

$$E = \int_{t_1}^{t_2} P(t)\mathrm{d}t \quad (9)$$

$$A = \pi R^2 \quad (10)$$

The thrust formula of the wind wheel and the wind speed correction formula under complex terrain are shown in equations (11) and (12):

$$T = \frac{1}{2}\rho C_T A V^2 \quad (11)$$

$$V_{\text{modified}} = V_{\text{free}} f(h, \theta, \lambda, \cdots) \quad (12)$$

The formula of turbulence intensity and the influence of terrain roughness on wind speed are shown in equations (13) and (14):

$$I = \frac{\sigma_V}{V_{\text{mean}}} \quad (13)$$

$$\frac{V_1}{V_2} = \left(\frac{z_1}{z_2}\right)^{\alpha} \quad (14)$$

3. Application of CFD in Wind Energy Development

Petersen et al. put forward the term "wind energy meteorology", which mainly refers to the application of meteorology, climatology and geography knowledge to deal with problems related to wind energy. Specifically, wind meteorology focuses on the climate change of the surface wind, mesoscale meteorological processes, microscale topography, and the impact of wind turbine arrangement, and wind turbine aerodynamics [16,17]. Due to the large research direction and spatial and temporal scale span of wind energy meteorology, these four aspects are traditionally developed by climatologists, meteorologists, wind engineering experts and aerodynamics experts in the corresponding field, and there is no connection between each other. Holtslag et al. believe that it is necessary to strengthen the communication between research fields and application fields and the integration of different disciplines. Due to the high Reynolds number turbulent motion in the atmospheric boundary layer, the influence of the complex underlying surface, and the interaction between the wind turbine motion and the atmospheric motion, the wind energy model is faced with a multi-scale, complex boundary and internal disturbance, and the flow problem needs to describe the flow process through the nonlinear dynamic model. With the scale development of the wind energy industry, the CFD model has been more and more used in the development and utilization of wind resources.

A. Meso-microscale Coupling Simulations

The development of wind energy is inseparable from the accurate understanding of the atmospheric boundary layer, especially the near-formation wind field. Further accurate simulation of the CFD microscale flow process is needed based on mesoscale numerical simulations of weather processes [18]. This process is increasingly used in wind energy assessment, micro location, and wind power prediction, known as the "downscaling" process, which changes from mesoscale to microscale.

In the process of "downscale", on the one hand, SOWFA simulator based on Open FOAM turbulence model, wind turbine model, boundary condition, etc. provides the interface between different scale for extending down to wind turbine scale; on the other hand, the mesoscale simulation results are used as flow condition to initialize the turbulence calculation on the microscale. If the flow does not contain all the flow scales that can be

distinguished by the microscale grid, it requires a certain transition distance to fully develop the turbulence, which is called the preheating process or the rotation process (Spin-up) [19,20]. However, this process is not an actual atmospheric motion and cannot be used to calculate wind power, etc. MMC has developed a method to accelerate the development of turbulence. It should be noted that this method is not suitable for unsteady flow.

Large scale and mesoscale atmospheric motion drive the horizontal uniform atmospheric boundary layer motion, terrain, vegetation, wind turbine wake to disturb the uniform flow, the real flow field is the sum of the average motion and disturbance [21,22]. Under ideal conditions, the change of uniform flow can be ignored, and the change of the atmospheric boundary layer is the result of the balance of turbulent viscosity stress, Coriolis force and horizontal pressure gradient force. Assuming the Coriolis force in the free atmosphere and the pressure gradient force, the ground rotating wind can be used to represent the pressure gradient as the upper boundary condition of the horizontal momentum equation. Under the assumption of positive pressure atmosphere (density is only a function of pressure), the change of ground rotating wind caused by horizontal temperature difference with height ("hot wind" or oblique atmosphere) can be ignored [23,24]. According to the Boussinesq approximation, in addition to the buoyancy term of the vertical component in the momentum equation, the density change can also be ignored (incompressible flow).

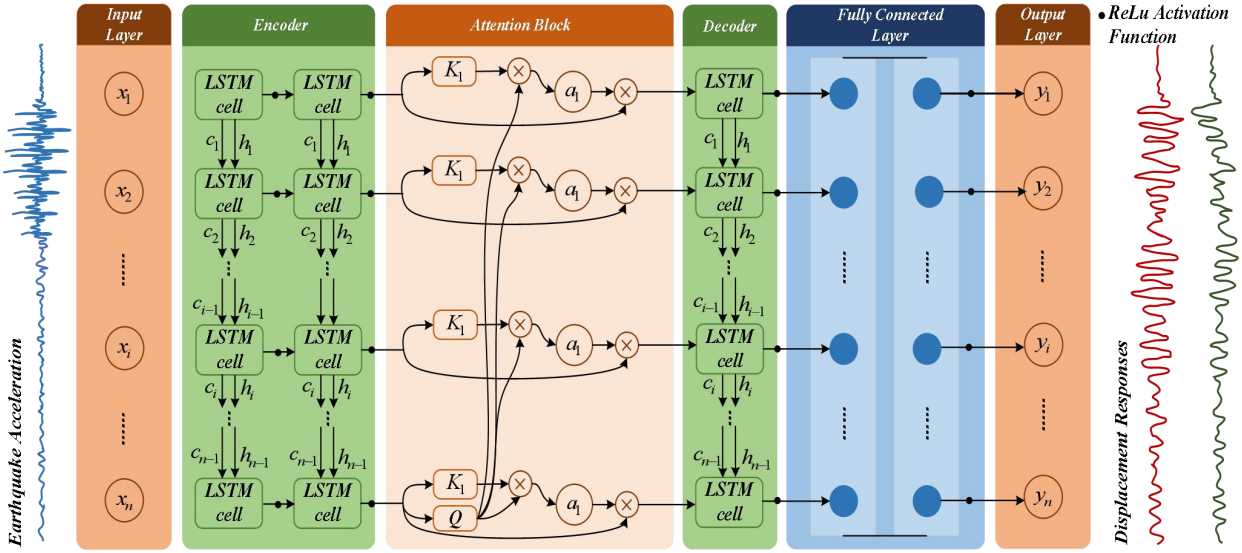

Figure 2. Turbulent flow closure scheme based on LSTM

Figure 2 shows the turbulent closure scheme based on LSTM. Based on different turbulent closure schemes, we connect the turbulent flux to the mean flow gradient to solve the mean flow equation on a one-dimensional grid. The first order closing (the 0 equation) uses the mixed length theory to parameterize the vortex viscosity coefficient; the first equation closing introduces the turbulent kinetic energy diagnostic equation, and the square root as the velocity scale to calculate the vortex viscosity coefficient; the second equation closing (second order) introduces the turbulent dissipation rate instead of the mixing length parameterization; the third order closing instead solves the isotropic vortex viscosity approximation. Considering the computational cost, the mesoscale atmospheric boundary layer parameterization and the wind engineering model generally choose the first-order or second-order turbulent closure scheme, which belongs to the moderate accuracy simulation compared to the third-order closure scheme or the LES model. The RANS model is developed by the research project for wind energy applications, and the wind field simulation driven by ideal boundary conditions are comparable to the LES results. For the real ABL wind field simulation, the average momentum of the WRF simulation is first used as the mesoscale forcing to drive the single column model, obtaining wind profile features similar to the WRF simulation, and second, the forcing terms in the momentum and heat equations are removed to quantify the influence of introducing different forcing mechanisms into the RANS model. The model can simulate the daily changes of night low jet and large scale forcing, ABL and the formation interaction, the results of the simulation including the surface flux and important wind variables, such as equivalent wind speed, wind turbine hub height wind direction, wind shear and wind direction, compared with Cabauw weather tower observation data, verify the accuracy of the simulation. This modeling approach from mesoscale to microscale is largely influenced by mesoscale input uncertainty. By introducing wind energy observations, the deviation from wind profile observations can be reduced.

B. Tail Flow Simulation

This research makes an important contribution to the optimization of renewable energy utilization by

developing a new optimization method based on CFD simulation results. Specifically, a high-precision wind field simulation system based on the coupling of mesoscale meteorological model and CFD software was studied to obtain high-resolution wind speed distribution data under complex terrain, and a differentiated wind turbine layout strategy for front, middle and back slopes was proposed, and the attenuation effect of terrain on wind speed was accurately evaluated through a unified quantitative method of wind speed baseline in open terrain. The developed optimization method can significantly improve the accuracy of wind energy resource assessment in complex terrain areas, and the error rate between the simulated wind speed and the actual data is controlled within 8%, and the annual power generation in a specific area can be increased by 30% by optimizing the wind turbine location and tower parameters. However, there is still a certain gap in the research: the current model is mainly carried out on typical mountain terrain, and if it is further incorporated into more complex terrain forms such as river valleys and cliffs, or combined with multi-factor coupling analysis such as vegetation cover and building disturbance, the research system can be more comprehensive, and the application boundary of CFD simulation under extremely complex geographical conditions can be further expanded, so as to provide more universal technical support for renewable energy development.

The interaction between wind turbines, atmospheric motion and complex terrain will produce a wake effect and reduce the wind power output [25,26]. In the process of downscaling, the atmospheric motion cannot be simply downscaled to the scale of the wind turbine, and the influence of the fan wake needs to be considered. For example, Sanderse et al. introduce various simulation methods of wind turbines, from the actuation disk model and the actuation line model based on the blade unit momentum theory to the direct simulation of wind turbines. Schulz et al. a direct simulation of the flow field of wind turbines based on the Spalart-Allmaras turbulence model [27]. Makridis And Chick used Fluent to study the wake and neutral atmospheric flow of complex terrain wind turbine, assumed the three-dimensional steady-state flow field, solved the RANS equation and Reynolds stress model, and the actuation disk model simulated the rotor effect, and verified the wind farm in flat terrain, hillside and coastal complex terrain. However, the engineering models are mostly used in these works. Until recently, the wind turbine modeling technology is still focused on the engineering models, such as the blade unit momentum theory and the speed loss model [28,29].

The vortex structure caused by the wind turbine begins to decompose, and the study of the aerodynamics of the blade is classified as the rotor model. Based on the N-S equation, the rotor and near-wake calculations can yield good results at about 10 m / s wind speed threshold. Compared with nonstationary RANS, LES can simulate higher resolution turbulence scale, which is important for the analysis of instationary blade load and wake evolution in wind turbine. For example, Jiminez et al. and Calaf et al. combine LES with actuation disk technology to simulate wake [30]. Although CFD wind turbine modeling improves the simulation accuracy, reliable inflow, blade paddle models and dynamic stall models are still needed to provide accurate blade load. Nanjing University of Aeronautics and Astronautics selected large scale wind turbine (NREL5MW) as the research object, and carried out numerical research on its different wake superposition effects through two forms of series and mistrain, obtained the distribution of mixed wake velocity and turbulence intensity, and analyzed the contribution items of turbulent kinetic energy TKE. FAST, a wind turbine model of the National Renewable Energy Laboratory, can calculate the aerodynamic forces, structural loadings, and power and control variables of the blades, and Storey etc. combine them with LES to calculate wind turbine performance, load, control response and wake.

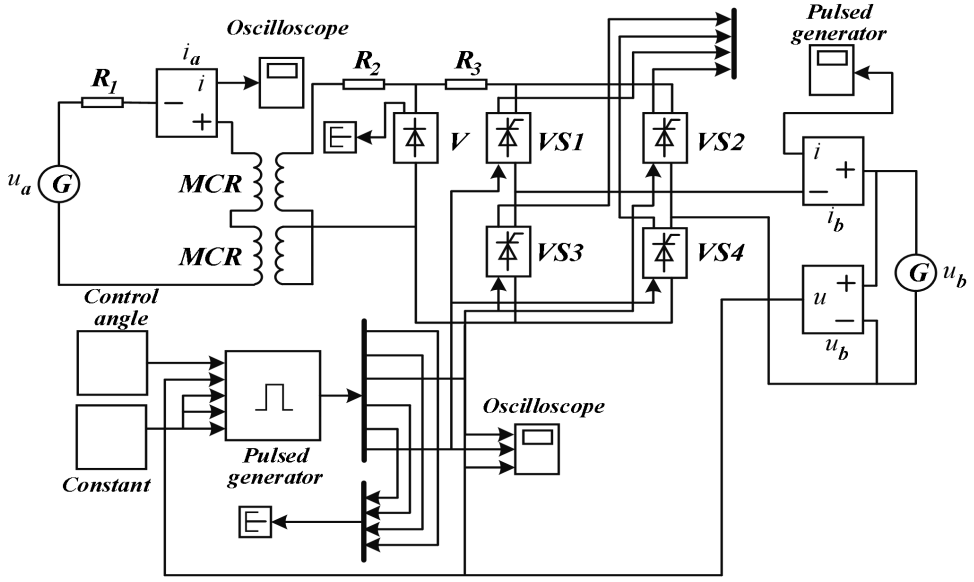

Figure 3. Internal circuit of the wind farm

This paper aims to create an optimized design tool for offshore wind farm. Figure 3 shows the internal circuit of wind farm, and its wake modeling improves the simulation ability of wind turbine wake. By comparing the simulation performance of Fuga, WRF, Actuator Disk / RANS, VENTOS, CFDWake, RANS / fpC, EllipSys3D and other models in terms of wind farm layout, wake loss and wind farm efficiency. The study found that the speed of the wind farm at the speed of the wind turbine is located at 80D~90D downstream of the wind turbine. The position of speed loss is not sensitive to the direction of inflow, and the maximum loss rate is 20%~25%. RANS model, mesoscale model and engineering model simulation results show that when the upstream wind field wake is downwind, there is a prominent triangular loss zone at 5D~10D, and the velocity decreases by 20%~30%. Due to the large uncertainty of the measurements, it is difficult to compare the merits of the model. Different models simulate the wake effect based on their own physical assumptions. These differences will also affect the simulation accuracy. With the increase of the wind farm scale, the prediction accuracy will be improved. Porte-Agel et al. detailed the interaction between wind turbine wake and wind farm wake and atmospheric flow, and pointed out the future research directions, such as the development of wind farm model with bidirectional coupling of wind turbine wake and atmospheric motion.

C. Wind Farm Simulation of Complex Terrain

More and more wind turbines are installed on hills, ridges or steep cliffs, and complex terrain is a problem for wind resource assessment. Wind energy assessment using statistical and linear models is reliable for flat terrain and can also simulate a gentle slope flow structure. For example, Finardi et al. reconstructed the wind field through linear interpolation to obtain the spatial distribution and height variation of the wind field to determine the position of the wind turbine; Lange and Højstrup predict the wind resources of offshore wind farms with WAsP near the Baltic Sea, which is very consistent with the observation results. However, the wind speed prediction is greatly biased when the wind speed area is in the longer area (when the wind surface, the wind speed and wind direction are basically the same). Moreover, for mountainous areas, linear models are significantly biased by the lack of important dynamic process description.

Recently, CFD simulation of complex terrain wind field has developed rapidly. Murakami, they developed the local wind field forecast system based on CWE, accurately predicted the local wind energy distribution with the new linear k- ε turbulence model and canopy model, and predicted the results of the undulating terrain of the two-dimensional ridge, mountain and subgrassland surface better than that of WAsP. Palma et al calculated with linear and CFD models in coastal areas and showed that CFD can simulate the separated flow well. Sadek et al. studied the performance of the linear diagnostic model (Flowstar) and the CFD model (Fluent) in simulating the effects of complex terrain, and found that the Fluent software simulation was more accurate, especially for the rear vortex of steep terrain. In order to improve the load of wind turbine load and long-term annual capacity estimation simulation accuracy, Vestas company provides more than 47 GW of wind turbine online real-time data, through the CFD of neutral near formation using two equation turbulence closed scheme (k- ε and k- ω) modeling forecast long-term annual capacity, shows that the results than the industry standard model WASP prediction has significant improvement. Based on this, Hristov et al. build a model suitable for the whole boundary layer of the atmosphere, including the Coreolis force and buoyancy, and weighted the specific layer junctions in the daily variation according to the frequency distribution of the mesoscale simulation to consider the heat transfer process. In the turbulent k- ε closure scheme of near formation, the flow diffusion is inflated because the turbulent mixing length increases monotonically with the height, thus adopting the k- ε CFD ABL model with the maximum mixing length restriction.

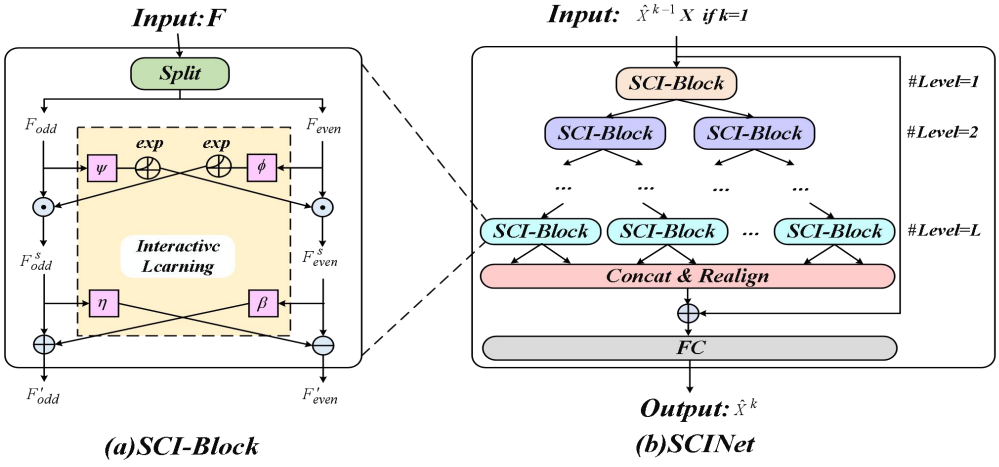

Figure 4. Simulation of complex terrain wind farm

Figure 4 is the simulation of complex terrain wind farm. Using CFD to simulate atmospheric flow in complex terrain is usually very time-consuming. For current processors, only parallel computing is enough to make

wind field prediction using CFD, where code operation evolves faster than real weather. Castro et al. used the parallel version of VENTOS CFD to successfully forecast the wind farm wind power, and combined with the mesoscale model to form a short-term prediction tool to simulate the Doro / Bustvid wind farm in the northern department of Portugal, showing the impact of parallel efficiency on the prediction. The CFD model developed by the Super Computing Center in Barcelona is based on the finite element high-performance parallel solver Alya. It uses Chimera method to refine the grid of the location of the wind turbine and the near wake area, and performs wind power prediction and wind farm optimization combined with meteorological data assimilation.

4. Experimental Results and Analysis

A. Characteristic Analysis of Wind Parameters on Mountain Slope

In engineering, the vertical terrain slope is generally not more than 45°, because too large a slope will adversely affect the stability of the wind field, construction and the operation of the wind turbine. In order to study the characteristics of wind parameters with different slopes, this paper selects the mountains of Inner Mongolia and the Shuangshan Mountains of Ganzhou as the objects, which are taken from the actual wind fields, and the slope extension lengths are different.

Considering the key influence of topography on the wind field simulation, the average altitude at the bottom of the mountain is selected as the zero point. In order to comprehensively and accurately analyze the wind field, a total of 20 locations were evenly selected along the horizontal and vertical directions on the mountain. In the horizontal direction, 5 points were selected at certain distances from the windward side to the leeward side of the mountain to capture the changes of wind parameters at different lateral positions. Vertically, from the bottom to the top of the mountain, 4 rows of points are selected at equal height intervals to study the wind characteristics of different height layers. The construction fan impeller has a diameter of 145 m and a hub design height of 90 m in IEC SB design.

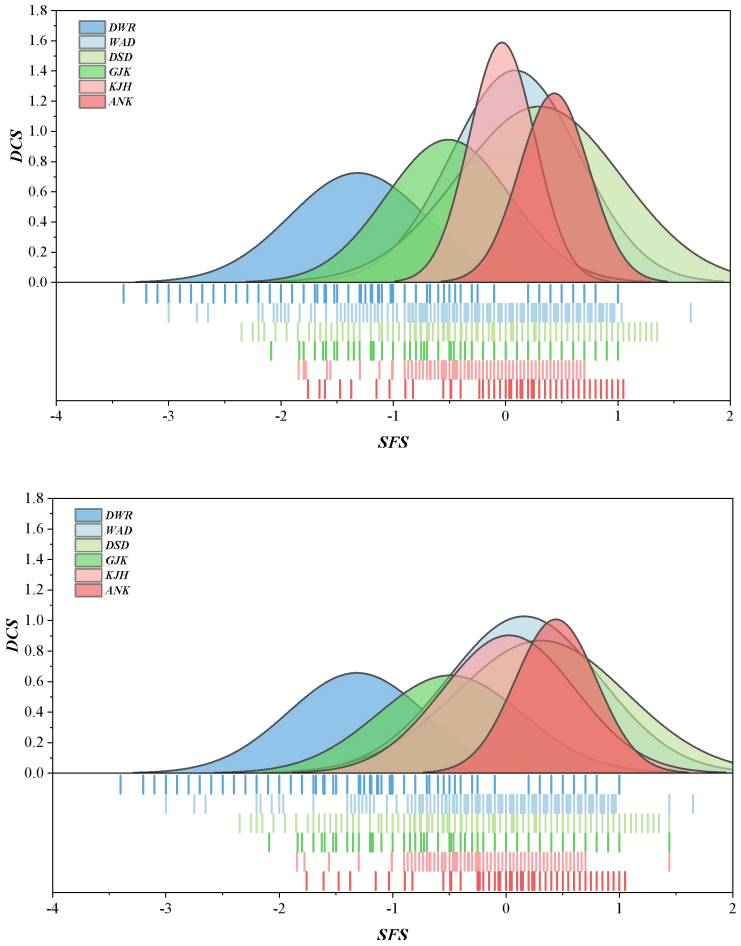

Figure 5. Characteristic analysis of slope wind parameters

Figure 5 shows the characteristic analysis of slope wind parameters, using H1, H2 and H3 to indicate the lower tip height, hub height and upper tip height. The flow wind along the front slope of the mountain has the acceleration effect, reaching the maximum at 3 positions at the peak of the mountain, and the vertical wind shear value at the peak is small or negative. The wake behind the mountain is greatly affected by the terrain, the wind speed in the low layer is very low, and the turbulence

intensity is large, so the lee side of the main wind direction of the mountain should be avoided.

B. Position-Selection Analysis

The construction of machine platform is limited by protection area, construction conditions, load safety and other conditions, so the vertical position can be divided into three conditions: front, middle and behind the slope. The common acceleration effect of the original terrain appears at the top of the mountain, and the slope neutral machine and the slope vertical machine show large flow separation at the plane position, and the flow separation area occupies a certain height. Only the slope maintains a gentle speed transition in the height direction of the position.

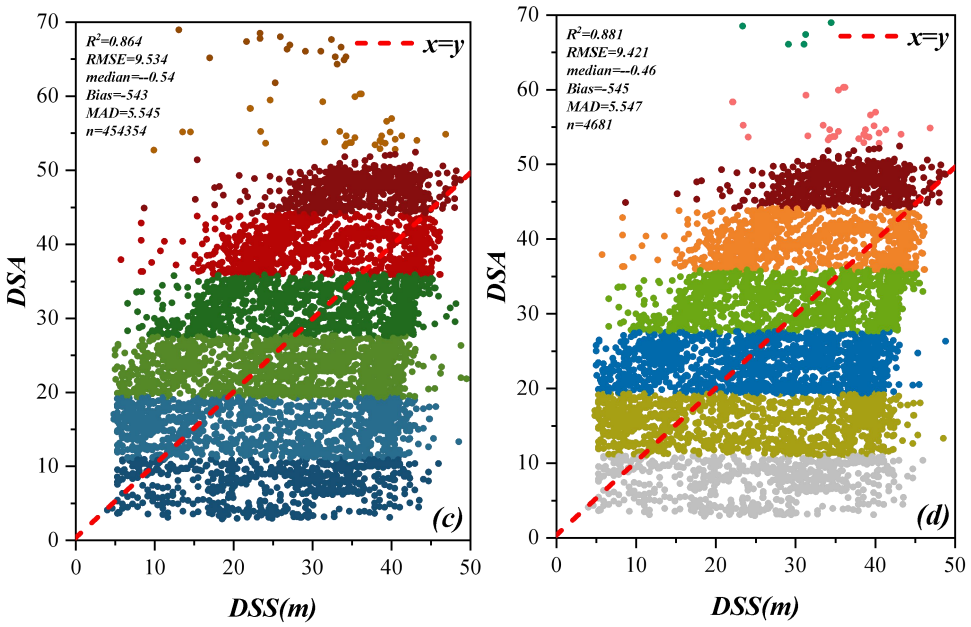

Figure 6. Analysis of vertical position feature distribution

Figure 6 presents the distribution analysis of vertical position characteristics, According to the experiment, The choice of different vertical positions affects the wind speed, The horizontal wind speed distribution of the slope is close to the original terrain, The height wind speed of the lower tip, the hub and the upper tip decreased by 7.7%, 0.6% and 0.2%, respectively, The wind speed of the lower tip, hub and upper tip decreased by 22.4%, 6.0% and 2.4% respectively, The wind speed of the lower tip, hub and upper tip of the rear eller decreased by 50%, 6.8% and 2.6% respectively, at the same time, The wind speed behind the slope changes sharply in the low altitude range, The shear value and the turbulence intensity are both too high. Therefore, in the construction of the station platform, the foundation platform should be built on the side close to the current direction.

C. Impact of Machine Position Excavation Depth

Hillside terrain to platform area and foundation stability to meet the requirements, usually increase the machine platform dig depth, this section in the same high slope slope, the machine platform dig height simulation calculation, excavation depth change, essentially changed the distance between the tip and slope, under the tip under the slope height, flow will be blocked by the slope.

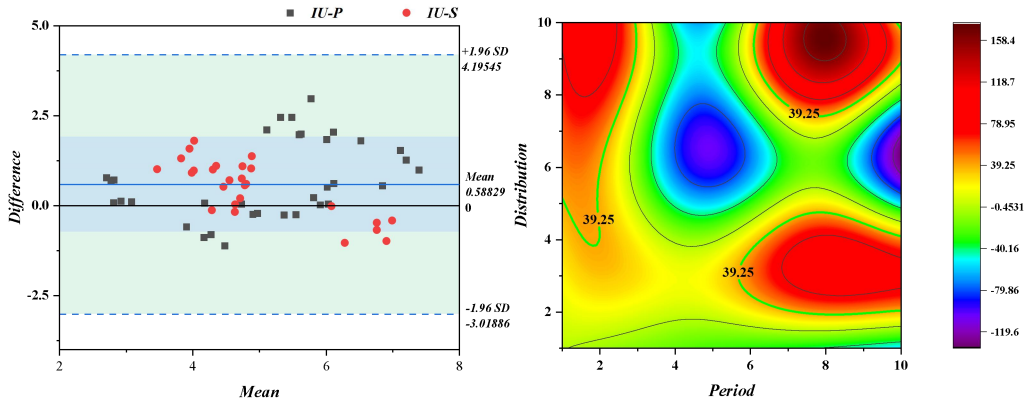

Figure 7. Impact analysis of machine position excavation depth

Figure 7 illustrates the analysis of the influence of machine excavation depth on sensitivity, particularly for the disk. As the digging depth increases, the distance to the bottom tip, the steepness of the high slope, and the potential for burial below the slope all become more pronounced, with wind speed being a significant factor. As depicted in Figure 7, when the lower tip is positioned below the slope, the hub height and the upper tip height increase, and the rate of wind speed reduction gradually levels off with depth. Considering the condition of the slope in front of the machine, if the wind originates from the back slope, the machine's position platform becomes more sensitive to the excavation depth. Additionally, the occlusion of the lower leaf tip can severely deteriorate the wind conditions on the lower disk surface of the unit.

5. Summarize

Fine simulations of wind turbines are becoming more mature, and more models are being improved, including CFD, ADM and ALM, and grid resolutions can reach between meters and tens of meters. Clearly, at such a resolution, the ALM and ADM models are inappropriate. As the wind turbine becomes higher and higher, the vertical grid resolution becomes more and more refined. Even in large-scale models, the vertical resolution near the surface can reach tens of meters, and the grid points fall within the height of the wind turbine. At this point, the effect of the wind turbine is usually represented by the physical strength acting on the grid point, where the average kinetic energy decreases and the turbulent kinetic energy increases. Through CFD simulation, the efficiency of renewable energy can be improved. Simulations in one region show that the region's wind power system is expected to generate 30 percent more electricity annually to 5,000 megawatt hours through optimal fan layout and tower parameters optimization. This data shows that the CFD simulation provides an important scientific basis and guidance for the optimization of renewable energy utilization.

Funding

This work was sponsored in part by China Yangtze Power Co.,Ltd. (Z532302051)

References

[1] D. Kiribuchi, T. Yoshida, F. Okayama, K. Konno, T. Matsuda. Development of a simulation-based optimization method for wind farm layout on complex terrain. IEEJ Transactions on Electronics Information and Systems, 2023, 143(2), 151-158. DOI: 10.1541/ieejeiss.143.151

[2] J. Decaix, M. Mettille, N. Hugo, B. Valluy, C. Muench-Alligne. CFD Investigation of the Hydraulic Short-Circuit Mode in the FMHL/FMHL plus Pumped Storage Power Plant. Energies, 2024, 17(2), 473. DOI: 10.3390/en17020473

[3] G.D. Han, N.Z. Zheng, J.M. Wu. Function optimization of ceramic firing process and reduction of energy consumption based on cfd simulation. Journal of Physics: Conference Seriesd. DOI: 10.1088/1742-6596/2729/1/012003

[4] S. Acarer, C. Uyulan, Z.H. Karadeniz. Optimization of radial inflow wind turbines for urban wind energy harvesting. Energy, 2020, 117772. DOI: 10.1016/j.energy.2020.117772

[5] Y. Ma, Y.Y. Zhu, A.M. Zhang, C. Hu, S. Liu, Z.Y. Li. Hydrodynamic performance of vertical axis hydrokinetic turbine based on taguchi method. Renewable Energy, 2022, 186. DOI: 10.1016/j.renene.2022.01.037

[6] M.M.G. Dias, R.G. Ramirez Camacho. Optimization of nrel phase vi wind turbine by introducing blade sweep, using cfd integrated with genetic algorithms. Journal of the Brazilian Society of Mechanical Sciences and Engineering, 2022, 44(2), 1-19. DOI: 10.1007/s40430-021-03357-y

[7] M. Ilic, V. Stefanovi, S. Pavlovi, G. Ili. Cfd analysis of temperature field in pellet stove as a generator of an absorption heat pump. Facta Universitatis Series Working and Living Environmental Protection, 2020, 163. DOI: 10.22190/FUWLEP2003163I

[8] Z. Cheng, F.S. Lien, E. Yee, H. Meng. A unified framework for aeroacoustics simulation of wind turbines. Renewable Energy, 2022, 188(3), 299-319. DOI: 10.1016/j.renene.2022.01.120

[9] S.Q. Wang, Y. Zhang, Y.Y. Xie, G. Xu, K. Liu, Y. Zheng. The effects of surge motion on hydrodynamics characteristics of horizontal-axis tidal current turbine under free surface condition. Renewable Energy, 2021, 170(1), 773-784. DOI: 10.1016/j.renene.2021.02.037

[10] X.H. Gao, S. He, Y.S. Gu. An efficient mode shape-based RBF mesh deformation approach via forward-backward greedy algorithm in CFD/CSD coupled simulation. Journal of Fluids and Structures, 2025, 133. DOI: 10.1016/j.jfluidstructs.2025.104276

[11] S. Shoeibi, S.A.A. Mirjalily, H. Kargarsharifabad, R. Dhivagar. Correction to: comparative study of doubleslope solar still, hemispherical solar still, and tubular solar still using al. Environmental Science and Pollution Research International, 2022, 29(43), 65370. DOI: 10.1007/s11356-022-20738-5

[12] J.X. Wang, X. Qin, S.X. Xin, G.C. Lu. The investigation of the optimization based on market mechanism to the operation of a thermal-wind-photovoltaic hybrid generation system. International Transactions on Electrical Energy Systems, 2021, 31. DOI: 10.1002/2050-7038.12621

[13] Q.G. Wang, J. Xu, K.Y. Wang, P. Wu, W.R. Chen, Z.R. Li. Parallel electromagnetic transient simulation of power systems with a high proportion of renewable energy based on latency insertion method. IET Renewable Power Generation, 2022, 17(1), 110-123. DOI: 10.1049/rpg2.12385

[14] J.Y. Li, H. Zhao. Multi-Objective Optimization and Performance Assessments of an Integrated Energy System Based on Fuel, Wind and Solar Energies. Entropy, 2021, 23(4), 431. DOI: 10.3390/e23040431

[15] Z.V. Zhang, W.Z. Wang, J. Lyu, X.B. Ke, C. Shao, J. Liu, et al. Increasing the Wind Power Utilization of Hybrid AC/DC Systems Based on Optimal Active Power Control of HVDC. 2020 International Conference on Smart Grids and Energy Systems (SGES), 2020. DOI: 10.1109/sges51519.2020.00041

[16] X. Wu, W.Z. Cui, Y.X. Wang, W.F. Xiang. Human thermal comfort in kitchen with different ventilation modes based on a coupled CFD and thermoregulation model. Journal of Building Engineering, 2024, 94. DOI: 10.1016/j.jobe.2024.110000

[17] S.N. Leloudas, G.N. Lygidakis, A.I. Eskantar, I.K. Nikolos. A robust methodology for the design optimization of diffuser augmented wind turbine shrouds.

Renewable Energy, 2020, 150, 722-742. DOI: 10.1016/j.renene.2019.12.098
[18] A. Khanjari, E. Mahmoodi, M.H. Ahmadi. Energy and exergy analyzing of a wind turbine in free stream and wind tunnel in cfd domain based on actuator disc technique. Renewable Energy, 2020, 160(2020), 231-249. DOI: 10.1016/j.renene.2020.05.183
[19] M. Tawfik, A.S. Shehata, A.A. Hassan, M.A. Kotb. Renewable solar and wind energies on buildings for green ports in egypt. Environmental Science and Pollution Research International, 2023, 30, 47602-47629. DOI: 10.1007/s11356-023-25403-z
[20] A. Saria, T. Tahar. Performance analysis of two gas turbine power plants with different air preheater design and numerical simulation of the performant regenerator. 2019 10th International Renewable Energy Congress (IREC), 2019. DOI: 10.1109/irec.2019.8754506
[21] E. Al Shami, Z. Wang, X. Wang. Non-linear dynamic simulations of two-body wave energy converters via identification of viscous drag coefficients of different shapes of the submerged body based on numerical wave tank cfd simulation. Renewable Energy, 2021, 179. DOI: 10.1016/j.renene.2021.07.068
[22] M. Zandsalimy, C. Ollivier-Gooch. Residual vector and solution mode analysis using semi-supervised machine learning for mesh modification and CFD stability improvement. Journal of Computational Physics, 2024, 510. DOI: 10.1016/j.jcp.2024.113063
[23] O.Y. Zhang, L. Yuan, X.R. Teng, F.F. Zhao, X. Fan, C.Y. Tao, et al. CFD-based investigation of flow field in a glass furnace reactor under an oxy-fuel electric boosting mode. Scientific Reports, 2025, 15(1). DOI: 10.1038/s41598-025-87261-8
[24] R. Daneshazarian, U. Berardi. Nano-enhanced thermal energy storage coupled to a hybrid renewable system for a high-rise zero emission building. Energy Conversion and Management, 2023, 291. DOI: 10.1016/j.enconman.2023.117301
[25] R. Chaabane, A. Jemni, N.A.C. Sidik, W.X. Xian. Numerical study of magneto-hydrodynamic free convection heat transfer and fluid flow. Technological Advancement in Mechanical and Automotive Engineering, 2023, 547-564. DOI: 10.1007/978-981-19-1457-7_43
[26] Y. Tao, Y.H. Yan, X. Fang, H.H. Zhang, J.Y. Tu, L. Shi. Solar-assisted naturally ventilated double skin facade for buildings: room impacts and indoor air quality. Building and Environment, 2022, 216, 109002. DOI: 10.1016/j.buildenv.2022.109002
[27] M. Upadhyay, A. Kim, S.S.S. Paramanantham, H. Kim, D.J. Lim, S.Y. Lee, et al. Three-dimensional cfd simulation of proton exchange membrane water electrolyser: performance assessment under different condition. Applied Energy, 2022, 306. DOI: 10.1016/j.apenergy.2021.118016
[28] N. Azimy, M.R. Saffarian, A. Noghrehabadi. Thermal performance analysis of a flat-plate solar heater with zigzag-shaped pipe using fly ash-cu hybrid nanofluid: cfd approach. Environmental Science and Pollution Research International, 2024, 31(12), 18100-18118. DOI: 10.1007/s11356-022-24640-y
[29] H. Amein, B.M. Akoush, M.M. El-Bakry, M. Abubakr, M.A. Hassan. Enhancing the energy utilization in parabolic trough concentrators with cracked heat collection elements using a cost-effective rotation mechanism. Renewable Energy, 2022, 181, 250-266. DOI: 10.1016/j.renene.2021.09.044
[30] D.S. Strebkov, N.S. Filippchenkova. Results of cfd-simulation of a solar photovoltaic-thermal module. IOP Conference Series: Earth and Environmental Science, 2021, 659(1), 012113. DOI: 10.1088/1755-1315/659/1/012113